Journal of Ceramic Processing Research. Vol. 13, No. 2, pp. 138~141 (2012)

J O U R N A L O F
Ceramic Processing Research

Properties and rapid consolidation of nanostructured FeAl-Al_2O_3 composites from mechanically synthesized powders by pulsed current activated sintering

In-Yong Ko[a], Seung-Hoon Jo[a], Jung-Mann Doh[b] , Bang-Ju Park[c], Jin-Kook Yoon[b] and In-Jin Shon[a,*]

[a]*Division of Advanced Materials Engineering and Research Center for Advanced Materials Development, Engineering College, Chonbuk National University, 664-14 Deokjin-dong 1-ga, Deokjin-gu, Jeonju, Jeonbuk 561-756, Korea*

[b]*Advanced Functional Materials Research Center, Korea Institute of Science and Technology, PO Box 131, Cheongryang, Seoul 130-650, Korea*

[c]*College of BioNano Tech., Gachon University, 1342 SeongnamDaero, Soojung-gu, Seongnam-si, Gyeonggi-do 461-701, Korea*

Nanopowder of FeAl and Al_2O_3 was synthesized from Fe_2O_3 and Al by high energy ball milling. A dense nanostuctured FeAl-Al_2O_3 composite was consolidated by a pulsed current activated sintering method within 3 minutes from mechanically synthesized powders of FeAl and Al_2O_3. The grain size, sintering behavior and hardness of the sintered FeAl-Al_2O_3 composite were investigated.

Key words: Mechanical alloy, Composite, Nanomaterials, Hardness, Rapid sintering.

Introduction

Iron aluminide (FeAl) is of interest for structural applications at elevated temperature in hostile environments. This is because it generally possess excellent oxidation and corrosion resistance, a relatively lower density and lower material cost than Ni-based alloys [1, 2]. However, its use has been limited by its brittleness at room temperature. This drawback can be improved by grain size reduction and the addition of second phase.

Conventional methods of processing iron aluminides, including casting, hot rolling and powder metallurgy, have been investigated [3, 4]. However, none of these methods yield nanostructures. Four decades ago, high energy ball milling and mechanical alloying of powder mixtures, were reported to be efficient techniques for the preparation of nanocrystalline materials and alloys.

Nanocrystalline materials have received much attention as advanced engineering materials with improved physical and mechanical properties [5, 6]. As nanomaterials possess a high strength, high hardness, excellent ductility and toughness, undoubtedly, more attention has been paid for their applications of nanomaterials [7,8]. In recent days, nanocrystalline powders have been developed by the thermochemical and thermomechanical process named the spray conversion process (SCP), by co-precipitation and high energy milling [9-11]. However, the grain size in sintered materials becomes much larger than that in pre-sintered powders due to a rapid grain growth during conventional sintering process. Therefore, although the initial particle size is less than 100 nm, the grain size increases rapidly up to 500 nm or larger during conventional sintering [12]. So, controlling grain growth during sintering is one of the keys to the commercial success of nanostructured materials. In this regard, the pulsed current activated sintering method which can make dense materials within 2 minutes, has been shown to be effective in achieving this goal [13, 14].

The purpose of this study is to produce mechanical synthesis of nanopowder of FeAl and Al_2O_3 and a dense nanocrystalline FeAl-Al_2O_3 composite within three minutes by using this pulsed current activated sintering method and to evaluate their mechanical properties and grain sizes.

Experimental Proceduer

Powders of 99% Fe_2O_3 (< 5 nm, Alfa, Inc) and 99% pure A1 (–200 mesh, Samchun Pure Chemical Co., Inc) were used as a starting materials. Fe_2O_3 and 4Al powders were mixed by a high-energy ball mill, Pulverisette-5 planetary mill at 250 rpm and for 10 h. Tungsten carbide balls (10 mm in diameter) were used in a sealed cylindrical stainless steel vial under an argon atmosphere. The weight ratio of ball-to-powder was 30:1. The grain sizes of FeAl and Al_2O_3 were calculated by Suryanarayana and Grant Norton's formula [15] :

$$B_r(B_{crystalline} + B_{strain})\cos\theta = k\lambda / L + \eta\sin\theta \quad (1)$$

where B_r is the full width at half-maximum (FWHM) of the diffraction peak after instrumental correction;

*Corresponding author:
Tel : +82 63 270 2381
Fax: +82 63 270 2386
E-mail: ijshon@chonbuk.ac.kr

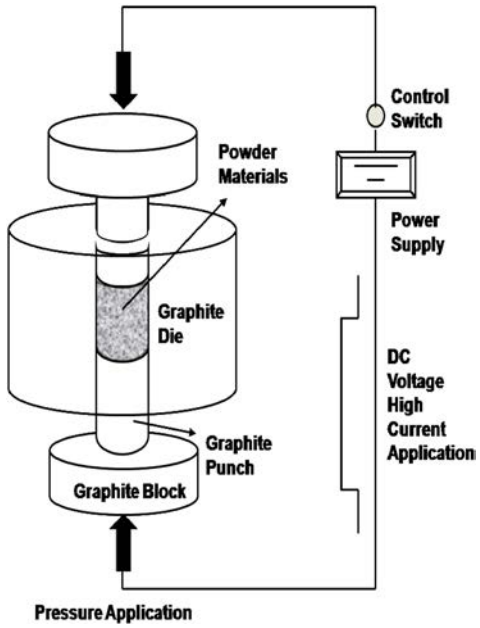

Fig. 1. Schematic diagram of apparatus for pulsed current activated sintering.

$B_{crystalline}$ and B_{strain} are the FWHM caused by the small grain size and internal strain, respectively; k is a constant (with a value of 0.9); λ is the wavelength of the X-ray radiation; L and η are grain size and internal strain, respectively; and θ is the Bragg angle. The parameters B and B_r follow Cauchy's form with the relationship: $B = B_r + B_s$, where B and B_s are the FWHM of the broadened Bragg peaks and a standard sample's Bragg peaks, respectively. After milling, the mixed powders were placed in a graphite die (outside diameter, 45 mm; inside diameter, 20 mm; height, 40 mm) and then introduced into the pulsed current activated sintering system made by Eltek in South Korea shown in Fig. 1. The four major stages in the sintering are as follows. The system was evacuated (stage 1). And a uniaxial pressure of 80 MPa was applied (stage 2). A pulsed current (on time; 20 μs, off time; 10 μs) was then activated and maintained until densification was attained as indicated by a linear gauge measuring the shrinkage of the sample (stage 3). The temperature was measured by a pyrometer focused on the surface of the graphite die. At the end of the process, the sample was cooled to room temperature (stage 4).

The relative densities of the synthesized sample were measured by the Archimedes method. Microstructural information was obtained from product samples which were polished and etched using a solution of H_2SO_4 (20 vol.%) and H_2O (80 vol.%) for 35 s at room temperature. Compositional and microstructural analyses of the products were made through X-ray diffraction (XRD) and scanning electron microscopy (SEM) with energy dispersive X-ray analysis (EDAX). Vickers hardness was measured by performing indentations at load of 20 kg and a dwell time of 15 s on the synthesized samples.

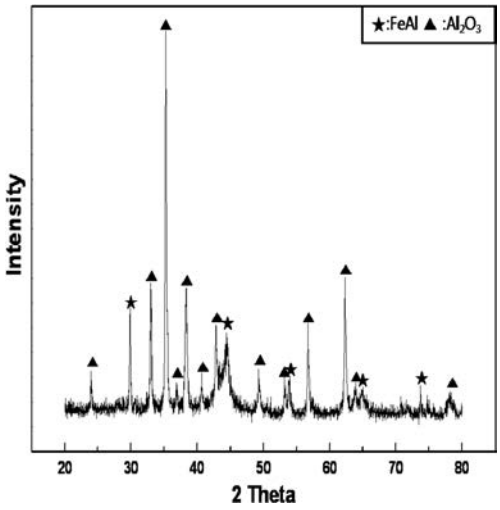

Fig. 2. XRD patterns of powder milled for 10 h.

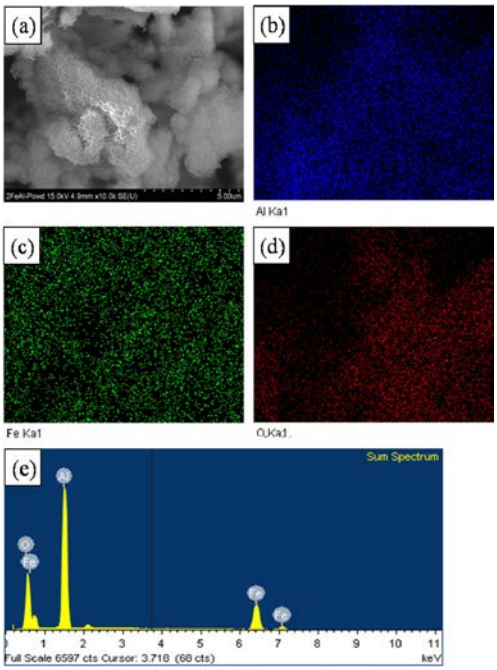

Fig. 3. Fe-SEM image (a), X-ray mapping (b), (c), (d) and EDS analysis (e) in high energy ball milled powders of Fe_2O_3-Al.

Result and Discussion

XRD patterns of the milled powder is shown in Fig. 2. Reactant powders of Fe_2O_3 and Al peaks are not detected but product powders of FeAl and Al_2O_3 are detected. Therefore, it is considered that mechanical synthesis is produced during the high energy ball milling. Fig. 3 shows an FE-SEM image, X-ray mapping and EDS ananlysis in the high energy ball milled powder of FeAl and Al_2O_3. In the FE-SEM image, the powders are very fine and agglomerated. Al and O are detected at the same point in the X-ray mapping and in EDS,

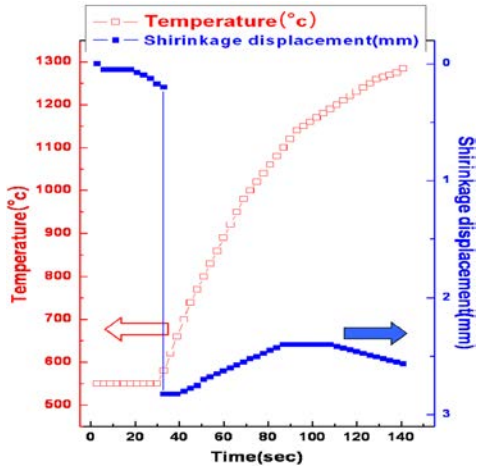

Fig. 4. Variations of the temperature and shrinkage displacement with heating time during pulsed current activated sintering of the FeAl-Al_2O_3 system.

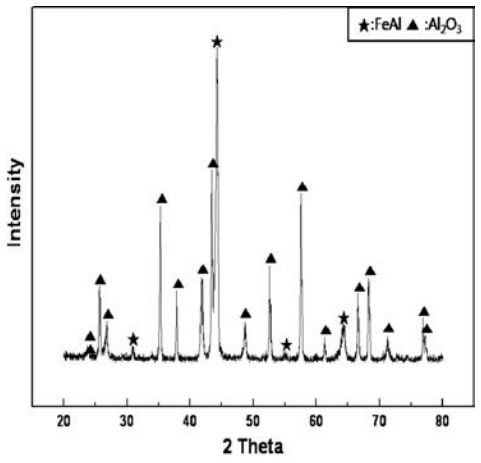

Fig. 5. XRD patterns of the FeAl-Al_2O_3 composite sintered at 1280 °C from high energy ball milled powder.

only Fe, O and Al peaks are detected. The average grain sizes of FeAl and Al_2O_3 measured by Suryanarayana and Norton's formula [15] were 4 and 57 nm, respectively.

The changes in shrinkage displacement and temperature of the surface of the graphite die with heating time during the processing of the FeAl and Al_2O_3 system are shown Fig. 4. As the pulsed current was applied, the shrinkage displacement of FeAl and Al_2O_3 continuously increased with temperature up to about 550 °C, and then abruptly increased. Fig. 5 shows XRD patterns of 2FeAl-Al_2O_3 composite sintered at 1280 °C. Only FeAl and Al_2O_3 peaks are detected. To calculate grain sizes of the FeAl and Al_2O_3 in the composite, $B_r\cos\theta$ versus $\sin\theta$ are shown in Fig. 6. The structural parameters, i.e. the average grain sizes of FeAl and Al_2O_3 measured by Suryanarayana and Norton's formula [15] are 48 nm and 60 nm, respectively. And the relative density of 2FeAl-Al_2O_3 composite is about 96%. Fig. 6 shows FE-SEM images for the FeAl-Al_2O_3 composite sintered

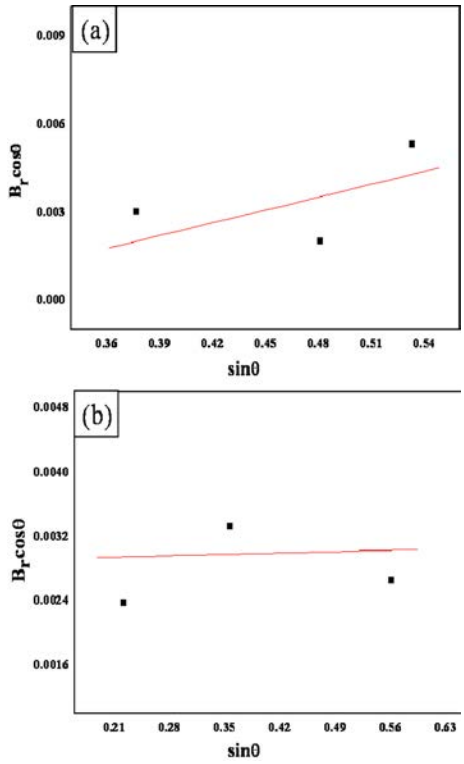

Fig. 6. Plots of $B_r\cos\theta$ versus $\sin\theta$ in FeAl (a) and Al_2O_3 (b) in the composite sintered at 1280 °C.

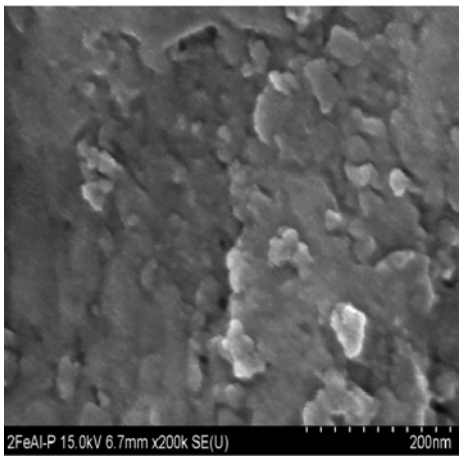

Fig. 7. FE-SEM image of the FeAl-Al_2O_3 composite sintered at 1280 °C.

from high energy ball milled powder. The composite consists of nanocrystalline material.

Vickers hardness measurements were made on polished sections of the 2FeAl-Al_2O_3 composite using a 20 kg_f load and 15 s dwell time. The calculated hardness values of the FeAl- Al_2O_3 composite sintered from high energy ball milled powder were 550 kg/mm^2. This value represents an average of five measurements. Cracks were not observed to propagate from the indentation corners. So, fracture toughness can not be calculated from crack length. Godlewska *et al*. investi-

gated FeAl sintered from self-propagating high-temperature synthesized powders followed by hot forging. The hardness and grain sizes of their FeAl were 274 kg/mm^2 and 24 (radial), 8.2 (axial) μm [16]. The hardness in this study is higher than that of Goglewska *et al.*'s study due to a refinement of the grain size and the addition of Al_2O_3.

Conclusions

Using the pulsed current activated sintering method, the densification of nanostructured 2FeAl-Al_2O_3 was accomplished from mechanically synthesized powder of FeAl-Al_2O_3. A nearly full density of 2FeAl-Al_2O_3 composites can be achieved within 3 minutes with an applied pressure of 80 MPa and the pulsed current. The average grain sizes of the FeAl and Al_2O_3 are 48 nm and 60 nm, respectively. And the relative density of 2FeAl-Al_2O_3 composite is about 96%. The calculated hardness values of FeAl-Al_2O_3 composite sintered from high energy ball milled powder were 550 kg/mm^2.

Acknowledgements

This work is partially supported by KIST Future Resource Research Program and by the Human Resources Development of the Korea Institute of Energy Technology Evaluation and Planning (KETEP) grant funded by the Korea government Ministry of Knowledge Economy (No. 20114030200060).

References

1. C.T. Liu, E.P. George, P.J. Maziasz, and J.H. Schneibel, Mater Sci Eng A 258 (1998) 84-98.
2. S.C. Deevi and V.K. Sikka, Intermetallics 4 (1996) 357-375.
3. V.K. Sikka, In Proceedings of the 5th Annual Conf. on Fossil Energy Materials (Oak Ridge, TN, 1991) p. 197
4. J.R. Knibloe, R.N. Wright, and V.K. Sikka, Advanceds in powder metallurgy, edited by E.R. Andreotti, P.J. McGreehan (Princeton, NJ: Metal powder Industries Federation, 1990) p. 219.
5. M.S. El-Eskandarany, J. Alloys & Compounds. 305 (2000) 225-238.
6. L. Fu, L.H. Cao, and Y.S Fan, Scripta Materialia. 44 (2001) 1061-1068.
7. K. Niihara, Elsevier Scientific Publishing Co. Trieste, Italy (1990).
8. S. Berger, R. Porat, and R. Rosen Progress in Materials. 42 (1997) 311-320.
9. Z. Fang and J.W. Eason, Int. J. of Refractory Met. & Hard Mater. 13 (1995) 297-303.
10. A.I.Y. Tok, L.H. Luo, and F.Y.C. Boey, Matrials Science and Engineering A. 383 (2004) 229-234.
11. S.L. Du, S.H. Cho, I.Y. Ko, J.M. Doh, J.K. Yoon, S.W. Park, and I. J. Shon, Kor. J. Met. Mater. 49 (2011) 231-235.
12. M. Sommer, W.D. Schubert, E. Zobetz, and P. Warbichler, Int. J. of Refractory Met. & Hard Mater. 20 (2002) 41-50.
13. N.R. Park, I.Y. Ko, I.J. Shon, K.T. Hong, J.M. Doh, S.H. Oh, and J.K. Yoon, Journal of Ceramic Processing Research 12 (2011) 534-537.
14. H.S. Kang, I.Y. Ko, J.K.Yoon, J.M. Doh, K.T. Hong, and I.J. Shon, Met. Mater. Inst. 17 (2011) 57-61.
15. C. Suryanarayana and M. Grant Norton, X-ray Diffraction A Practical Approach, p. 213, Plenum Press (1998).
16. E. Godlewska, S. Szczepanik, R. Mania, J. Krawiarz, and S. Kozinski, Intermetallics 11 (2003) 307-312.